

- Technical Paper -

SEISMIC BEHAVIOR OF COMPOSITE EWECs COLUMNS WITH VARYING SHEAR-SPAN RATIOS

FAUZAN^{*1}, Hiroshi KURAMOTO^{*2}, Tomoya MATSUI^{*3} and Ki-Hyung KIM^{*4}

ABSTRACT

Results of an experimental study on seismic behavior of Engineering Wood Encased Concrete-Steel (EWECs) composite columns with varying shear span to depth ratios (shear-span ratios) are summarized. Three specimens were tested under constant axial load and lateral load reversals. The column cross-section was kept constant while the column height was varied to produce different shear-span ratios. The results showed that the maximum flexural strength of the columns increased with decreasing shear-span ratio. However, more damages on the columns were observed with decreasing shear-span ratio.

Keywords: column, composite structures, woody shell, shear-span ratio, seismic test

1. INTRODUCTION

Composite steel-concrete columns such as Steel Reinforced Concrete (SRC) and Concrete Filled Tube (CFT) columns have been widely used in high-rise and long-span buildings. Many types of new composite columns have been developed in recent years. One of them is Engineering Wood Encased Concrete-Steel (EWECs) column [1,2], consisting of concrete encased steel (CES) core and an exterior woody shell, as shown in Fig. 1.

Some benefits are realized from this type of composite column due to the use of woody shell as column cover. The benefits of using woody shell in EWECs columns include the improved structural behavior through its action to provide core confinement and resistance to bending moment, shear force and column buckling, and the reduced construction cost because the woody shell also acts as forming for concrete placement. These advantages make EWECs columns possible to apply to actual structures as an alternative to SRC columns, which have weaknesses due to difficulty in constructing both steel and reinforced concrete (RC) [3].

A comprehensive research program has been underway for the last two years to construct the rational models of EWECs columns by investigating the seismic performance. In an earlier phase of the research program, the authors

studied the seismic behavior of an EWECs column using double H-section steel, which was compared with that of CES column without cover concrete, which corresponds to the core of the EWECs column [1]. It was found that the EWECs column had a stable spindle-shaped hysteresis characteristic without capacity reduction until the maximum story drift angle, R of 0.05 radian. The results also showed that the presence of woody shell on EWECs columns contributed to flexural capacity by around 12 %.

Recently, in the second phase of the research program, EWECs columns using single H-section steel have been studied with different types of woody shell connection at column-stub joints [2]. From this study, excellent hysteretic performance and damage limit were reported for EWECs columns with column-stub connection consisting of woody shell and wood panel attached to stub.

To complement the research program, test on EWECs columns with varying shear span to depth ratio ranging from 1.0 to 2.0 under constant axial load and lateral load reversals were performed. This paper discusses the effects of shear span to depth ratio on the seismic behavior of EWECs columns. In this paper, the shear span to depth ratio hereafter referred to as "shear-span ratio". The findings of this research contribute to the information needed to construct the guidelines for seismic design of EWECs structures.

*1 Graduate Student, Dept. of Arch. & Civil Eng., Toyohashi Univ. of Technology, MSc.E., JCI Member

*2 Associate Prof., Dept. of Arch. & Civil Eng., Toyohashi Univ. of Technology, Dr.E., JCI Member

*3 Research Associate, Dept. of Arch. & Civil Eng., Toyohashi Univ. of Technology, Dr.E., JCI Member

*4 Graduate Student, Dept. of Arch. & Civil Eng., Toyohashi Univ. of Technology, JCI Member

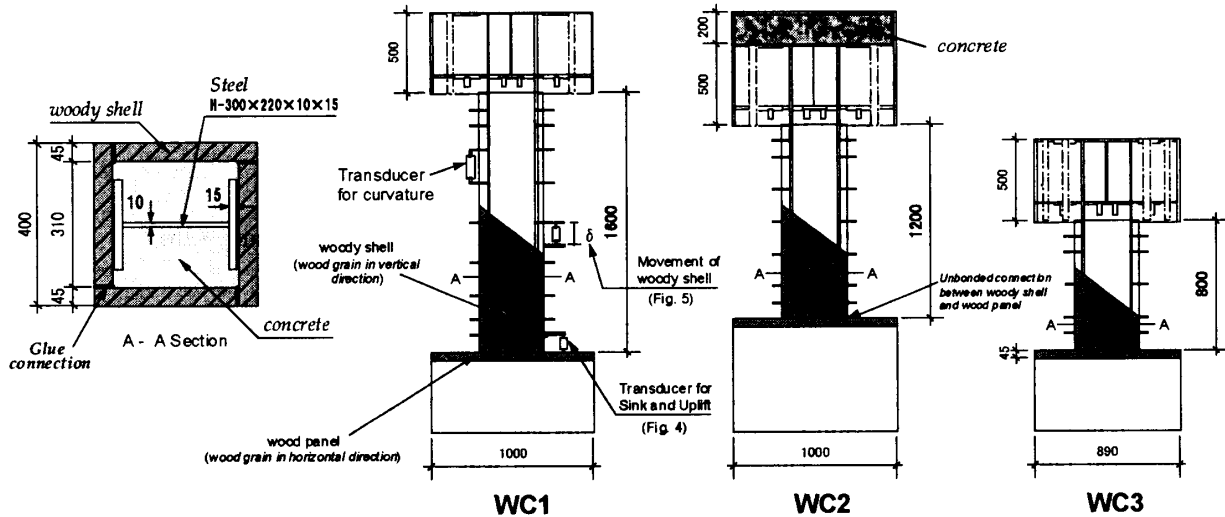


Fig.1 Test specimen

2. EXPERIMENTAL PROGRAMS

2.1 Specimens and Materials Used

A total of three composite column specimens of which the scale is about two-fifth, with varying shear-span ratios were tested. The column cross-section was constant at 400 mm square section for all specimens and different shear-span ratios (1.0, 1.5 and 2.0) were achieved by varying the column height (800mm, 1200mm and 1600mm). The dimensions and details of the specimens are shown in Fig. 1 and Table 1. The column-stub connection consisting of woody shell and wood panel attached to stub were constructed for all specimens (see Fig. 1). For Specimen WC2, the upper and lower stubs were filled by concrete with 200 mm height (Fig. 1), to reach the same elevation with Specimen WC1 in order to make easier to setup the specimen in the loading apparatus.

The steel encased in each column had a single H-section steel of 300x220x10x15 mm and the thickness of the woody shell for all specimens was 45 mm. The mechanical properties of the steel and the woody shell are listed in Tables 2 and 3, respectively. Normal concrete of 27 MPa was used for all specimens. The mix proportions and properties of the concrete are given in Table 4.

In manufacturing the specimens, the steel sections were accurately cut to size of the column and stub first. Then the woody shell panels were assembled to the column by using epoxy (Fig. 1). Finally, the concrete was cast into the column

Table 1 Test program

Specimen		WC1	WC2	WC3
Shear span to depth ratio		2.0	1.5	1.0
Woody Shell Thickness (mm)		45		
Concrete		Normal Concrete		
Steel	Built-in steel (mm)	H-300 x 220 x 10 x 15		
Column Height: h (mm)		1600	1200	800
Cross section: b x D (mm)		400 x 400		
Axial Compression	N (kN)	1031		
	N/(N _{tot})	0.18		

N_{tot} is the total axial compressive strength of the column (b_c · D_c · σ_B + b_w · D_w · σ_w).
 b_c · D_c · σ_B: the width, depth and compressive strength of concrete core
 b_w · D_w · σ_w: the width, depth and compressive strength of woody shell

Table 2 Mechanical properties of steel

Steel	Yield Stress σ _y (MPa)	Max. Stress σ _s (MPa)	Notes
H-300x220x10x15	284	450.5	Flange
	295.5	454.9	Web

Table 3 Mechanical properties of woody shell

Wood type	^a Comp. Strength σ _w (MPa)	Elastic Modulus E _s (GPa)
Glue laminated pine wood	45.0	11.5

^a the direction is parallel to axis of grain

Table 4 Mix proportions and mechanical properties of concrete

W/C (%)	S/(S+G) (%)	Slump (cm)	Unit weight (kg/m ³)					Comp. Strength MPa
			Water (W)	Cement (C)	Sand (S)	Gravel (G)	Admixture (A)	
57	48	17	181	318	856	989	3.18	27

Table 5 Calculated strength

Specimen		WC1	WC2	WC3
Q _{mcal} (kN)	Fiber Section Analysis	716.5	804.1	942.7
	Superposition Method	712.3	904.7	1091

Q_{mcal}: Calculated ultimate flexural strength

without additional formwork because the woody shell serves as mold forms for concrete placement.

The ultimate flexural strengths for each column shown in Table 5 were calculated by using two methods: fiber section analysis (FSA) and flexural analysis with superposition method. The detail of the FSA procedures is given in Ref. [4]. In the superposition method, it is assumed that all materials contribute its maximum compressive strength. In addition, no tensile force in the woody shell was assumed due to the unbonded connection between woody shell and wood panel at the column-stub joints (Fig. 1).

2.2 Test Setup and Loading Procedures

Figure 2 schematically illustrates the test setup and loading apparatus for this test. The specimens were loaded lateral cyclic shear forces by a horizontal hydraulic jack and a constant axial compression of 1031 kN by two vertical hydraulic jacks. Considering the cross section of the woody shell, the applied axial force ratio, $N/(b_c D_c \sigma_B + b_w D_w \sigma_w)$ for all specimens was 0.18 (Table 1), while using the core area, the ratio, $N/(b_c D_c \sigma_B)$ was 0.43.

The loads were applied through a steel frame attached at the top of a column that was fixed to the base. The two vertical jacks applying the constant axial compression were also used to keep the column top beam parallel to the bottom beam so that the column would be subjected to anti-symmetric moments. For Specimen WC3, the additional steel boxes at the top and bottom of the column stubs were used to connect the loading

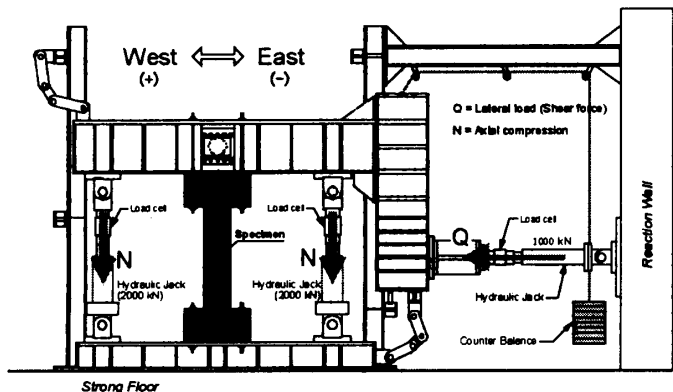


Fig.2 Schematic view of test setup

frames and the stubs, as shown in Photo 1.

The incremental loading cycles were controlled by story drift angles, R , defined as the ratio of lateral displacements to the column height, δ/h . The lateral load sequence consisted of two cycles to each story drift angle, R of 0.005, 0.01, 0.015, 0.02, 0.03 and 0.04 radians followed by half cycle to R of 0.05 radian.

3. TEST RESULTS AND DISCUSSIONS

3.1 Hysteresis Characteristics and Failure Modes

Shear versus story drift angle relationships of all specimens are plotted in Fig. 3. The dotted and chained lines drawn in these figures represent the calculated flexural strengths by fiber section analysis and superposition method, respectively. The yield and maximum strengths and the corresponding story drift angles for each specimen are listed in Table 6. The yielding of each specimen was assumed when the first yielding of steel flange and/or web at the top and bottom of the columns was observed, which corresponds to a triangle mark on the shear versus story drift angle response (Fig. 3). Crack modes of all specimens at R of 0.05 rad. are presented in Photo 2.

From Fig. 3, it can be seen that all specimens showed ductile and stable spindle-shaped hysteresis loops without degradation of load-carrying capacity until story drift, R of 0.05 rad. for Specimen WC1 and R of 0.03 rad. for the other two specimens.

In Specimen WC1 with a shear-span ratio of 2.0, the first yielding occurred on steel flange when the applied load was 386 kN and R of 0.005 rad. Within a drift ratio of 0.03 rad., the first cracks in the woody shell occurred in the North side of the column face at around 30 cm away from the top of the column. Moreover, the cracks extended along the column height with an increase of the story drift angle. Sink and uplift were



Photo 1 Specimen WC3 during testing

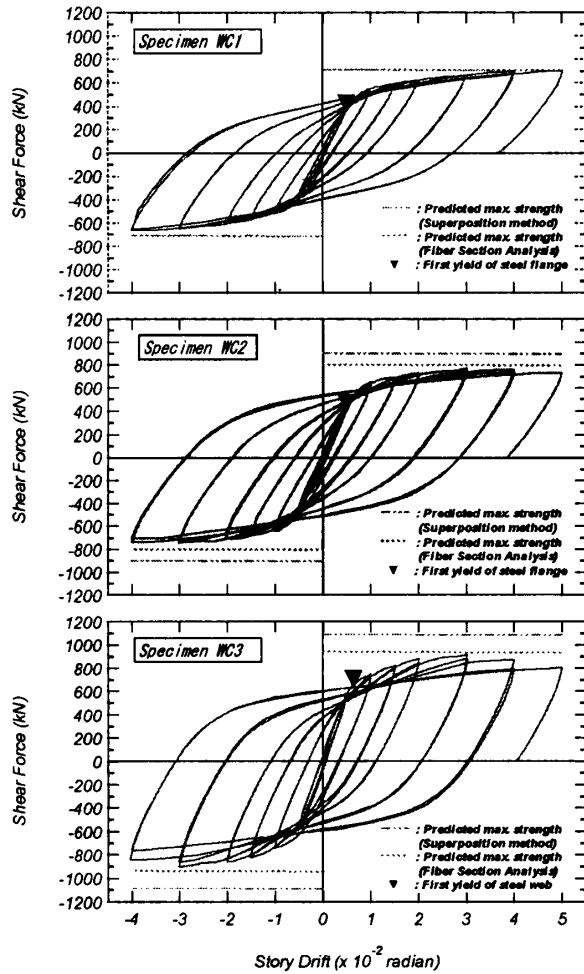


Fig.3 Shear force - story drift relationships

Table 6 Measured strength

Specimen	at Yielding		at the Max. Capacity	
	Qy (kN)	Ry (rad.)	Qmax (kN)	Rmax (rad.)
WC1	386	0.005	706.5	0.05
WC2	423.1	0.005	771.9	0.03
WC3	666.2	0.0064	916	0.03

observed significantly after R of 0.02 rad. at two opposite sides of both the top and bottom of the column due to different wood grain directions (different strengths and stiffnesses) between the woody shell and the wood panel attached to the stub. The hysteresis loops of this specimen showed excellent behavior without strength degradation until the last story drift, R of 0.05 rad., where the maximum capacity of 706.5 kN was reached.

For Specimen WC2 with a shear-span ratio of 1.5, the first yielding also occurred on steel flange at shear force of 423.1 kN and R of 0.005 rad. The first cracks of woody shell occurred at R of 0.02 rad. in the East side of the column. Subsequently, the cracks extended along the

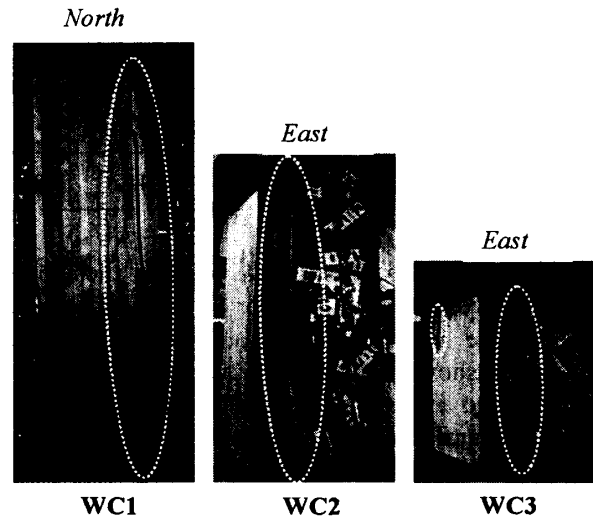


Photo 2 Crack modes of specimens at R = 0.05 rad. after loading

column height with the increase of story drift angle. The hysteresis curve showed a stable behavior with a little strength degradation after attaining the maximum capacity of 771.9 kN at R of 0.03 rad. The maximum capacity of this specimen was higher than that of Specimen WC1.

Specimen WC3 with the smallest shear-span ratio showed the highest maximum capacity among the tested specimens. A similar crack process with Specimen WC2 was observed for this specimen. However, the yielding location of this specimen was different from the other two specimens. The first yielding of the specimen occurred on the steel web at shear force of 666.2 kN and R of 0.0064 rad. The maximum capacity was reached at shear force of 916 kN and R of 0.03 rad.

By comparing the hysteresis loops of these specimens, it was revealed that the specimen strengths significantly increased with decreasing the shear-span ratio. This indicates that the shear-span ratio has a significant influence on the flexural strength of EWECs columns. In addition, the shear-span ratio also affects the yield location of the steel in which the first yielding of specimen with the smallest shear-span ratio occurred on the steel web due to the higher shear force.

From test results, it was found that the shear-span ratio also greatly affected the observed cracking patterns of the woody shell at the column faces. Up to story drift, R of 0.02 rad., no damage was observed in Specimen WC1 while small cracks occurred in Specimens WC2 and WC3 in the East side of the columns. The cracks of the woody shell in Specimen WC1 occurred in the North side of the column after R of 0.03 rad. Moreover, the cracks extended with increasing

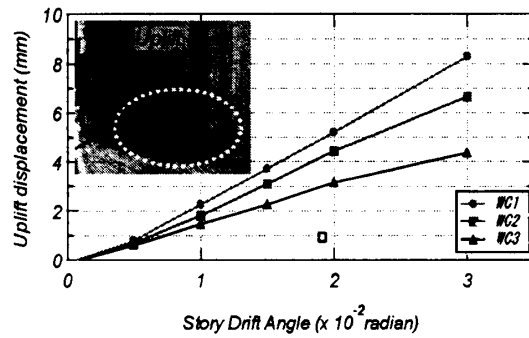
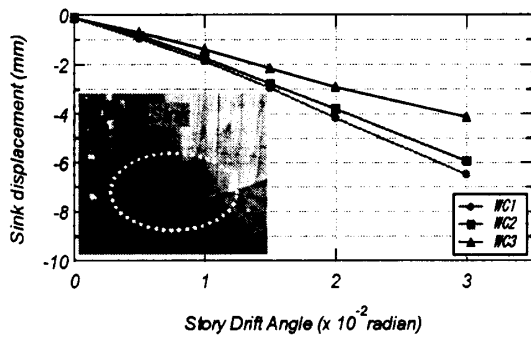


Fig.4 Sink and uplift displacements of woody shell at column-stub joint

story drift angle. Finally, the woody shell was split along the column height for all specimens, as shown in Photo 2. From the photo, it can be seen that Specimen WC3 with the smallest shear-span ratio had the most damages in which the cracks of the woody shell occurred in both East and North sides of the column. This indicates that the damage of woody shell becomes dominant with decreasing the shear-span ratio.

Figure 4 shows a comparison of sink and uplift of the woody shell at the column-stub joint at each story drift angle for all specimens. The values were obtained by measuring the vertical displacement between woody shell and wood panel at the joint using transducers (see Figs.1 and 4). The positive values represent the uplift displacements (tension) and negative values indicate the sink displacements (compression). It can be seen from the figure that the shear-span ratio affected the sink and uplift of woody shell at the joints. The sink and uplift displacements of woody shell at the joints increased with increasing the shear-span ratio.

Figure 5 compares the movement of the woody shell from the CES core until R of 0.02 rad. for all specimens. The values were obtained by measuring the displacement between the CES core and the woody shell using vertical transducers installed at the encased steel and the woody shell at the top, middle and bottom of the column, as shown in Fig. 1. The positive values represent the movements in the upward direction and negative values indicate the movements in the downward direction. The influence of the shear-span ratio on movement of the woody shell from the CES core of the columns is clearly seen in Fig. 5 in which the movement of the woody shell increased with decreasing the shear-span ratio.

After the test, the woody shell was removed from the columns to visually inspect the damage. It was observed for all specimens that the in-filled concrete had crushed in flexure at both the top and bottom of the column, and no local buckling occurred at the encased steel. In addition, shear

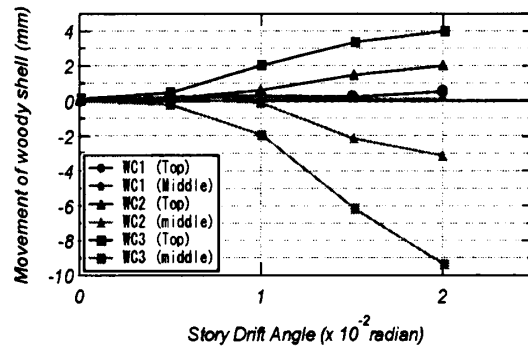


Fig.5 Movement of woody shell from CES core

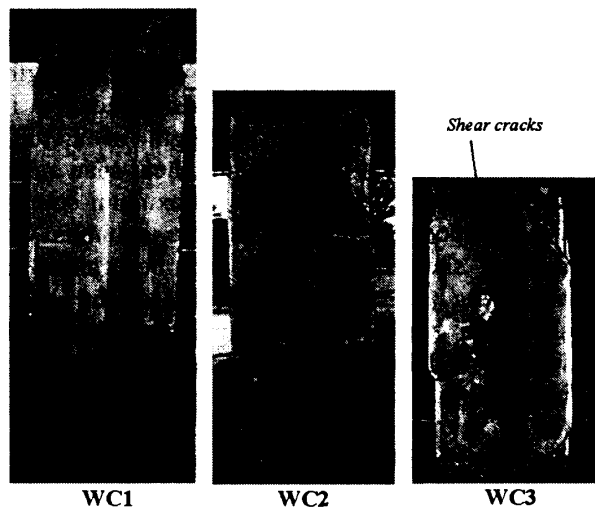


Photo 3 Crack patterns of CES cores after extracting the woody shell

cracks occurred along the column height in Specimen WC3 and no shear cracks was observed for the other two specimens, as shown in Photo 3.

3.2 Ultimate Strength

Figure 3 also shows the comparison between the measured and calculated maximum strengths. From the figure, it can be seen that the calculated flexural strengths by fiber section analysis fairly agreed with the measured maximum flexural strengths for all specimens. However, the calculated results by superposition

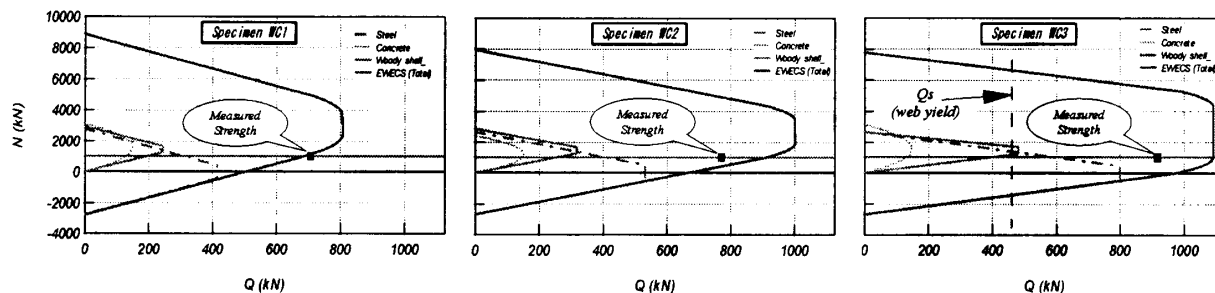


Fig.6 N-Q interaction curves of specimens calculated by superposition method

method showed a good agreement only for Specimen WC1 while for other two specimens, the results showed higher strengths than those of experimental results. The comparative results between the measured and calculated strengths by superposition method can also be seen in the N-Q interaction curves shown in Fig. 6.

The reason for the discrepancy between measured and calculated strengths by superposition method is that the method assumes that the woody shell contributes its maximum compressive strength, while it seems that the compressive stresses in woody shell did not reach the yield stress (σ_w), as described in the schematic uniaxial stress-strain curves in Fig. 7.

Based on the comparisons of the experimental and predicted maximum strengths, the fiber section analysis is recommended for predicting the maximum strength of EWECS columns including the varying shear-span ratios. The accuracy of the predicted maximum strength by superposition method for the columns with smaller shear-span ratios will be gained by modifying the stress-strain model of the woody shell. An appropriate constitutive model of the woody shell for the superposition method should be developed in the future research.

4. CONCLUSIONS

Based on the experimental study presented here, the following conclusions can be drawn:

- (1) A smaller shear-span ratio led to a higher shear force for the composite columns. The ultimate flexural strength of EWECS columns increased with decreasing the shear-span ratio.
- (2) The damage of the columns in the woody shell and the CES core became dominant with decreasing the shear-span ratio.
- (3) The calculated maximum flexural strengths by fiber section analysis were in good agreement with the test results while the superposition method results were greater than the observed strengths for the columns with smaller shear-span ratios. Modifications of the woody

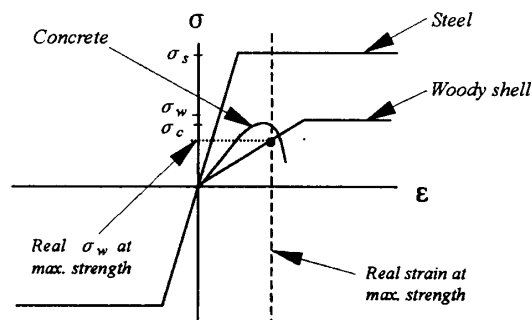


Fig.7 Schematic uniaxial stress-strain curves

shell constitutive model are needed to obtain the accuracy of calculation strength for EWECS columns by superposition method, especially for the columns with smaller shear-span ratios.

REFERENCES

- [1] Fauzan, Kuramoto, H., Shibayama, Y. and Yamamoto, T., "Structural Behavior of Engineering Wood Encased Concrete-Steel Composite Columns," Proceedings of JCI, Vol.26, No.2, 2004, pp. 295-300.
- [2] Fauzan, Kuramoto, H. and Kim, K-H., "Seismic Performance of Composite EWECS Columns using Single H-steel," Proceedings of JCI, Vol.27, No.2, 2005, pp. 307-312.
- [3] Kuramoto, H., Adachi, T. and Kawasaki, K., "Behavior of Concrete Encased Steel Composite Columns Using FRC," Proceedings of Workshop on Smart Structural Systems Organized for US-Japan Cooperative Research Programs on Smart Structural Systems (Auto-Adaptive Media) and Urban Earthquake Disaster Mitigation, Tsukuba, Japan, 2002, pp. 13-26.
- [4] Fauzan, and Kuramoto, H., "Experimental and Analytical Study on Structural Performance of Engineering Wood Encased Concrete-Steel Composite Columns," Proceedings of the Third International Conference on ASEM, Seoul, Korea, September, 2004, pp. 1447-1459.